Review Article

Anatomical and functional imaging in endocrine hypertension

Vikas Chaudhary, Shahina Bano[1]

Department of Radiodiagnosis, Employees' State Insurance Corporation (ESIC) Model Hospital, Gurgaon, Haryana, [1]Department of Radiodiagnosis, Lady Hardinge Medical College and Associated Smt. Sucheta Kriplani and Kalawati Hospitals, New Delhi, India

ABSTRACT

In endocrine hypertension, hormonal excess results in clinically significant hypertension. The functional imaging (such as radionuclide imaging) complements anatomy-based imaging (such as ultrasound, computed tomography, and magnetic resonance imaging) to facilitate diagnostic localization of a lesion causing endocrine hypertension. The aim of this review article is to familiarize general radiologists, endocrinologists, and clinicians with various anatomical and functional imaging techniques used in patients with endocrine hypertension.

Key words: Computed tomography, endocrine hypertension, magnetic resonance imaging, radionuclide imaging, ultrasound

INTRODUCTION

Hypertension is one of the common chronic diseases affecting one-fourth of the world population.[1] The true incidence and prevalence of hypertension with endocrine etiology are unknown. However, primary aldosteronism, the most common form among endocrine causes, is reported in 5–15% of all patients with hypertension. Overall, an endocrine contribution to high blood pressure may be present in more than 10% of cases.[2] EH is a term assigned to states in which hormonal derangements result in clinically significant hypertension. The majority of EH relates to adrenal disorders due to excess production of mineralocorticoids (primary hyperaldosteronism), catecholamines (pheochromocytoma), and glucocorticoids (Cushing's syndrome).[3] Other causes include growth hormone excess (acromegaly), primary hyperparathyroidism, and hyperthyroidism. The availability of anatomical and functional imaging techniques has tremendously changed the diagnostic approach to EH in clinical practice and has increased the interest of both radiologists and endocrinologists in this topic.

In the diagnostic work-up of EH, the anatomical and functional imaging techniques are used in synergistic manner. The anatomical imaging technique is used to locate, identify, and differentiate the different types of adrenal and other lesions causing EH, whereas the functional imaging is useful in characterizing and confirming the lesion.

DISCUSSION

Anatomical and functional imaging for mineralocorticoid-dependent hypertension

Computed tomography (CT) is the imaging modality of choice for evaluating adrenal gland morphology and masses associated with it. High-resolution CT of upper abdomen, using 1–3 mm thick slices to reduce volume averaging, is the most accurate technique for identifying adrenal lesions. Contrast-enhanced CT and delayed images help in further characterization of the lesions. The two main causes of primary hyperaldosteronism (Conn's syndrome) are aldosterone-producing adrenal adenoma (APA) and bilateral adrenal hyperplasia (BAH) of the zona glomerulosa that may, at times, be micronodular or macronodular. APAs were

Corresponding Author: Dr. Vikas Chaudhary, Department of Radiodiagnosis, Employees' State Insurance Corporation (ESIC) Model Hospital, Gurgaon-122 001, Haryana, India. E-mail: dr_vikaschaudhary@yahoo.com

previously thought to represent approximately two-third of cases of primary aldosteronism and BAH approximately one-third cases; however, recent evidence suggests that this ratio is reversed.[3] On CT scan, aldosterone-producing adrenal adenomas (APAs) usually appear as small (<4 cm in size), homogenous, well-circumscribed masses with smooth margin. Calcification, necrosis, and hemorrhage are uncommon in benign adenomas. A large amount of intracytoplasmic lipid within the adenoma allows for a quantitative evaluation by measuring the attenuation value of the lesion.[4] An attenuation value of 10 HU (Hounsfield units) or less on unenhanced image is diagnostic of adrenal adenoma [Figure 1], with 79% sensitivity and 96% specificity, and no further investigations are required. However, 30% adenomas are lipid-poor showing the attenuation value greater than 10 HU. A contrast-enhanced CT is required for further characterization of these lesions. A dynamic (at 60 s) and delayed (at 10 min) contrast-enhanced CT scan is obtained, a region of interest is drawn over the adrenal mass, and the attenuation is measured in Hounsfield units at 60 s and at 10 min. Then the percentage of contrast agent washout is calculated using formula [1 - (attenuation at 10 min/attenuation at 60 s)] X 100, where the attenuations are in Hounsfield units. The washout is a measurement of the percentage decrease between the initial enhancement and the delayed enhancement. A washout of greater than 50% is specific for benign adrenal adenoma, and a washout of less than 50% is specific for metastasis or malignancy. Thus, the contrast-agent washout measurement yields 98% sensitivity and 100% specificity and can reliably determine if an adrenal mass is benign or malignant.[5,6] In addition, we should always remember that nonfunctioning, incidental adrenal adenomas (incidentalomas) are commonly encountered on routine CT scans used for general abdominal imaging. Therefore, the diagnosis of primary hyperaldosteronism cannot be made on imaging result alone but must be correlated with biochemical testing.[7] In general, "a rule of four" has been suggested for incidentalomas,

which states that some 4% of CT scan reveals an adrenal incidentaloma (a mean across all ages); some 4% of these are either pheochromocytomas or adrenocortical cancers. A diameter of 4 cm is used to initiate mandatory removal and, finally, the current recommendation of follow-up is four years.[8] Moreover, in primary hyperaldosteronism, discriminating bilateral adrenal hyperplasia (BAH) from an aldosterone-producing adenoma (APA) is important because adrenalectomy, which is usually curative in APA, is seldom effective in BAH. Treatment for BAH is strictly medical. Unfortunately, no single test has been identified to fulfill this need. Moreover, the patients with BAH can have asymmetric adrenal macronodules, whereas some patients with APA may have tumor nodule too small (<5 mm) to be resolved even on high resolution CT scans. Thus, patients with bilateral nodularity or normal-appearing adrenal glands on CT should be referred to for adrenal vein sampling (AVS).[9]

Magnetic resonance imaging (MRI) of the adrenals is recommended in patients who are either allergic to the contrast media or in whom CT is contraindicated. MR parameters should include T1- and T2-weighted sequences along with chemical shift imaging. The signal intensity of an adrenal adenoma on T2-weighted image is usually lower than or similar to that of liver; whereas, adrenal metastases and carcinomas contain large amount of fluid than adenomas and thus demonstrate increased T2-signal intensity. However, there is significant overlap in T2 signal intensity between adrenal adenomas and metastases, rendering signal intensity an unreliable tool to differentiate between these two entities.[10] Chemical shift imaging, an MRI technique, which detects lipid within a lesion can be used to diagnose adrenal cortical adenomas with 81–100% sensitivity and 94–100% specificity.[11] Chemical shift imaging (in-phase and out-of-phase imaging) depends on the different resonance frequency rates of protons in fat and water molecules. Protons in fat are less susceptible to the external magnetic field and thus resonate at a slower
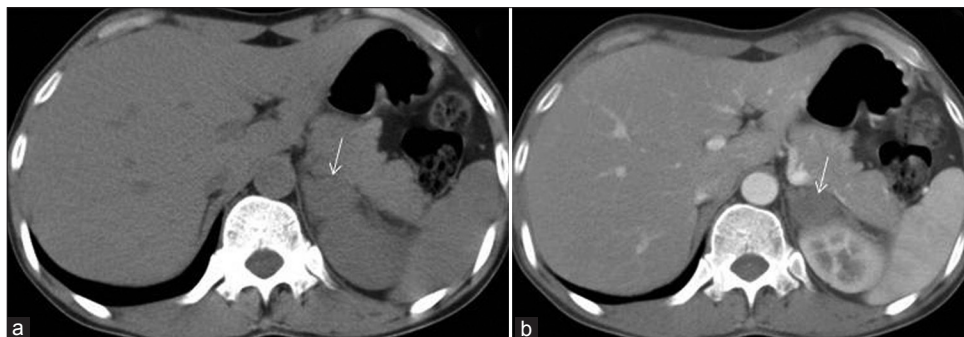

Figure 1: Atypical adrenal adenoma. A 45-year-old female with primary hyperaldosteronism due to left aldosterone-producing adenoma. Unenhanced CT image (a) shows ~ 4-cm size soft tissue density nodule in left adrenal gland (arrow). Limbs are not enlarged. Contrast-enhanced CT image (b) shows minimal enhancement of the nodule. The diagnosis of adenoma was confirmed on histopathological examination

frequency. The net effect of resonance of protons in fat and water molecules result in signal dropout in out-of-phase images relative to that in in-phase images. Thus, on out-of phase images, adenomas appear darker than on in-phase images, whereas metastases or carcinomas (because of lack of lipid and presence of water) appear bright on both in-phase and out-of-phase images.[12] Moreover, it should be noted that even MRI cannot be used to definitely characterize lipid-poor adenomas.

Stealth CT/MRI is a new imaging tool that uses a special computer system (stealth station) for image-guided surgeries in brain and spine. In brain, it enables surgeons to perform difficult brain (deeply located tumors, for example, pituitary microadenomas) and sinus surgeries with more safety and precision. In this technique, patient's CT or MRI scans of the brain (with small surface markers referred to as fiducials) are obtained prior to the surgery and imported into the stealth work station computer that compares the images to several anatomical landmarks or reference points on the patient's head and face. The computer then generates three-dimensional images of the patient's head, including surface fiducial markers and internal anatomy that are displayed on a high-resolution monitor in the operating room. Meanwhile, a sensor above the operating table tracks the position of the surgical instruments, which emits infrared light signals, and the computer calculates the position of the tip of the instrument and displays that location in a real-time fashion on the computer screen. The advantage of this technology is that (i) it allows the surgeons to determine the optimum trajectory to a tumor and plan operative approach to avoid eloquent brain tissue, (ii) it helps surgeon to obtain a real-time readout of his/her position during surgical procedure, aiding in more complete removal of the tumor while avoiding injury to sensitive structures and decreasing the incidence of postoperative neurological deficits, (iii) it is useful for directing needle biopsies, (iv) it also reduces the length of surgical procedure time and patient's hospital stay.[13]

Nuclear medicine imaging (NMI) is primarily a problem solving modality for lesions not adequately characterized even with CT and MRI. Adrenal cortical scintigraphy is a non-invasive technique for the functional characterization of adrenal lesions with overall sensitivity of 71–100% and specificity of 50–100%. Although, scintigraphy is rarely used in the diagnostic work-up of primary aldosteronism (PA) because of the relatively high radiation dose and its questionable sensitivity, but it can be useful to determine whether the abnormality is unilateral or bilateral. ^{131}I-6-β-iodomethyl-noncholesterol (^{131}I-NP-59) and ^{75}Se-selenomethyl-19-norcholesterol are two tracers used that bind to specifically low-density lipoproteins and are stored in the adrenocortical intracellular lipid droplets. Normal adrenals are visualized 5 days after the injection of the tracers. Unilateral adrenal uptake seen before 5 days suggests a functioning adenoma of greater than or equal to 2.0 cm size. The contralateral gland is not visualized because it becomes hypofunctional and atrophic due to prolonged ACTH suppression by autonomous cortical secretion from adrenal adenoma. Bilateral adrenal visualization before 5 days suggests adrenal gland hyperplasia. In general, hypersecreting tumors (e.g., aldosterone, cortisol, and androgen secreting adenomas) and nonhypersecreting adenomas show radiocholesterol uptake, whereas primary and secondary adrenal malignancies appear as "cold" nodules. Incidentalomas may show different radiocholesterol uptake patterns related to their nature and functional status.[10,14-16]

Anatomical and functional imaging for glucocorticoid-dependent hypertension

Hypertension is one of the most distinguishing features of Cushing's syndrome. Cushing's syndrome (CS), a hormonal disorder of excess cortisol production can often be quite challenging to diagnose. The disease is broadly classified into two group, that is, ACTH-dependent or ACTH-independent Cushing's syndrome. In both ACTH-dependent and ACTH-independent CS patients, CT, and/or MRI is the primary imaging modality for localization of the lesion, while scintigraphy is a useful confirmatory imaging method. ACTH-dependent Cushing's syndrome accounts for about 80% of all cases and is either due to a ACTH secreting pituitary adenoma (common) or extrapituitary neoplasm with ectopic ACTH production (uncommon). Ectopic sources of ACTH derive from a diverse group of tumor types that are more common in men after age of 40-years. Among these small-cell lung carcinoma and carcinoid tumors (bronchial, pancreatic, thymic, and disseminated), medullary thyroid carcinoma and pheochromocytoma tend to predominate; other less common causes include pancreatic carcinoma, gall bladder carcinoma, colonic carcinoma, and mesothelioma. Imaging of pituitary is an important part of the investigation of ACTH-dependent Cushing's syndrome to identify a possible pituitary lesion. The pituitary tumors in CS are usually microadenomas, which are 10 mm or less in diameter. Macroadenomas (>10 mm) are uncommon in patients with CS. MRI is the method of choice for evaluation of pituitary tumors. Modern MRI techniques using T1-weighted spin echo and/or spoiled gradient recalled acquisition (SPGR) techniques will identify an adenoma in up to 80% of patients with Cushing's disease. On MRI, 95% of microadenomas exhibit a hypointense signal with no postgadolinium enhancement [Figure 2]; however, remaining 5% have an isointense signal on postgadolinium scan. CT scan is less sensitive
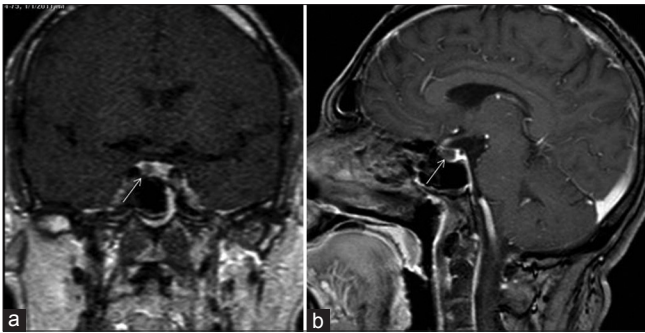
Figure 2: Pituitary microadenoma. A 30-year-old male with features of Cushing's syndrome due to pituitary microadenoma. High-resolution dynamic contrast-enhanced T1-weighted coronal (a) and sagittal (b) images of brain (at 60 s) show a small nonenhancing (dark) microadenoma (arrow) lateralized to right side of the pituitary gland. The normal pituitary gland shows marked homogenous enhancement

(40–50%) and inferior to MRI in detecting pituitary microadenomas, and it should be therefore reserved for patients in whom MRI is contraindicated or unavailable. CT imaging typically shows a hypodense lesion that fails to enhance postcontrast.[17-19] Unfortunately, normal-appearing pituitary may occur in some patients with Cushing disease due to both diffuse hyperplasia of ACTH-producing cells and small microadenomas that are not detected on imaging studies. In the latter case, ACTH lateralization during an inferior petrosal sinus sampling (IPSS) study may be useful in lateralizing the occult lesion and in guiding surgical therapy.[20] In one study, IPSS could correctly localize the lesion in 23 of 34 patients of Cushing's disease, giving a sensitivity of 67.6%, and picked up all the four patients with ectopic Cushing's syndrome and one with adrenal carcinoma, thereby giving 100% specificity.[21] PET scanning helps to monitor the efficacy of treatment in patients with pituitary adenoma, particularly when the tumor size seems unchanged or there is need to decide on the course of a drug regimen. Chest and abdominal CT scans should be performed in patients with suspected ectopic ACTH production. Somatostatin scintigraphy may also be helpful in detecting ectopic ACTH tumors, as majority of ectopic ACTH secreting tumors are of neuroendocrine origin and typically have cell surface receptors for somatostatin.[22] Conversely, the ACTH-independent Cushing's syndrome (adrenal Cushing's) is always caused by primary adrenal disease that secretes excess cortisol; it results from an adrenal adenoma (including adenoma within myelolipoma) and adrenal carcinoma accounting for 92% of cases, but rarely may be caused by bilateral adrenal hyperplasia (micronodular or macronodular).[17,18,23] Cross-sectional imaging (CT and MRI) appearance of cortisol-secreting adrenal adenoma is similar to that of APA, being relatively small (<5 cm), homogenous, and ovoid, with features consistent with intracellular lipid. Adrenocortical carcinoma is a rare, highly malignant tumor affecting patients with a median age of

about 43-years. Typical imaging features include large size at presentation, heterogeneous contrast enhancement, intratumoral calcification, hemorrhage, and necrosis. The majority of affected patients have metastatic disease (to lung and liver) at presentation; tumor invasion of IVC is also commonly reported.[24,25] On scintigraphy, in adrenal carcinoma, adrenal glands are not visualized bilaterally. These neoplasms do not accumulate sufficient tracer for visualization on scintigraphy.[26] Bilateral micronodular and macronodular adrenal hyperplasia have characteristic imaging features. On cross-sectional imaging, bilateral micronodular adrenal hyperplasia, also known as primary pigmented nodular adrenal dysplasia (PPNAD) typically shows normal appearing adrenal glands with multiple small nodules of 2–5 mm size.[27] Whereas, in bilateral macronodular adrenal hyperplasia, also known as ACTH-independent macronodular adrenal hyperplasia (AIMAH), both glands are grossly enlarged and contains relatively larger nodules measuring up to 5 cm in diameter.[28] Iodine-131-labelled adrenal scintigraphy in patients with bilateral nodular adrenal hyperplasia (PPNAD and AIMAH) show bilateral increased uptake.[26] Most cases of PPNAD occur as part of the Carney complex (CNC). CNC is a familial multiple neoplasia and lentigines syndrome associated with (i) PPNAD, (ii) hyperpigmentation of skin, and (iii) a variety of nonendocrine (myxomas of the heart, skin or breast) and endocrine tumors (growth hormone producing pituitary adenoma, testicular Sertoli cell tumor, Leydig cell tumor, and adrenal rest tumors). Cushing's syndrome occurs in approximately 30% of cases of CNC.[29]

Anatomical and functional imaging for catecholamine-dependent hypertension

Phaeochromocytoma (PH) is an important but rare cause of endocrine hypertension, occurring in about 0.1–0.9% of hypertensive individuals. PHs are rare neuroendocrine tumors of chromaffin tissue, most commonly found in adrenal medulla. These tumors produce excessive amounts of catecholamines (noradrenaline, adrenaline), responsible for paroxysmal hypertension. Approximately, 90% of PHs occurs within the adrenal glands, while 10% are located outside the adrenal glands (extra-adrenal) at various locations in the body. Extra-adrenal PHs are also known as paragangliomas. About 10% of the tumors are malignant, and substantial proportions (up to 25%) of apparent sporadic pheochromocytomas occur as part of familial syndromes, including MEN2 and VHL.[30] A combination of anatomical and functional imaging studies yield a sensitivity of nearly 100% for diagnosing these catecholamine-producing neoplasms. CT and MRI are generally indicated as primary imaging modalities for localization of these tumors. Sensitivities vary between 75% and 100% depending on location at adrenal or extra-

adrenal sites and whether the tumor is primary, recurrent, or metastatic. Both imaging methods have poor specificity. However, MRI is more sensitive than CT in detecting extra-adrenal pheochromocytomas (paragangliomas), and is considered as the anatomic imaging of choice because of its excellent anatomic detail, potential for better tissue characterization and multiplanar image capability.[31] PHs are usually 2–5 cm in diameter, solid, hypervascular masses, frequently with central necrosis, hemorrhage, and calcification. On MRI, most PHs are hypointense on T1-weighted images and markedly hyperintense on T2-weighted and fat suppressed T2-weighted images; however, low signal PHs (>30%) may be encountered at T2-weighted imaging. PHs commonly show avid but inhomogeneous enhancement after intravenous administration of contrast material [Figure 3]. Rarely, PHs may contain sufficient fat or may demonstrate rapid contrast washout and be mistaken for an adenoma at CT or MRI. Ten percent of PHs are found to be malignant; but unfortunately, the anatomic imaging features cannot sufficiently discriminate between benign and malignant PHs. Metastatic spread is the only reliable criterion for diagnosis of malignant PHs. Skeleton, lymph nodes, lung, and peritoneum are the most common sites for metastases. Iodine-131 or ^{123}I metaiodobenzylguanidine (MIBG) scintigraphy has 100% specificity but limited sensitivity (87%) and spatial resolution in detecting PHs. Single-photon emission scanning with [123I] metaiodobenzylguanidine improves both sensitivity and spatial resolution.[32] Radionuclide scanning is often useful when clinically suspected PHs (i.e., extra-adrenal lesions) cannot be localized by imaging techniques and particularly for metastatic PHs. Somatostatin receptor scintigraphy with octreotide, an analogue of somatostatin, can also localize PHs, but in less than 30% cases. In present scenario, ^{18}F-fluoro-2-deoxy-D-glucose (^{18}F-FDG) or ^{18}F-fluorodihydroxyphenylalanine (^{18}F-DOPA)-PET is the most commonly used functional imaging technique in clinical practice to detect and localize

PHs. PHs usually show increased uptake on ^{18}F-FDG or ^{18}F-fluorodihydroxyphenylalanine PET scans.[33-35] The sensitivity of [18]FDG-PET scanning is about 70% and that of ^{18}F-fluorodihydroxyphenylalanine about 100% for detecting solitary pheochromocytoma.[33,34] The newly introduced ^{68}Ga-DOTA radiopharmaceuticals for PET/CT imaging are particularly useful to detect more malignant lesions.[36]

Anatomical and functional imaging in acromegaly

Acromegaly due to pituitary gland involvement is uncommon but important cause of EH. Pituitary macroadenomas (75%) are more frequent than microadenomas (25%) in patients with acromegaly. MRI of sella is the investigation of choice for evaluation of growth hormone-secreting pituitary adenoma [Figure 4].[37] MRI is also preferred for postsurgical surveillance. Imaging with chest and abdominal CT to detect rare extracranial GHRH-secreting tumor is only indicated if pituitary MRI is normal and there is a definitive biochemical evidence of acromegaly. Intraoperative high-field magnetic resonance imaging with integrated microscope-based navigation is one of the most sophisticated techniques in pituitary tumor surgery. It provides a reliable immediate intraoperative control and helps to localize hidden tumors that otherwise would be overlooked.[38] Somatostatin-receptor scintigraphy (SRS) with 111In-DTPA-D-Phe-octreotide (111In-octreotide), in combination with other imaging modalities is useful in the diagnosis and follow-up of pituitary tumors, particularly GH-secreting tumors than in other adenomas. It distinguishes recurrent or residual tumor from postsurgical scar/necrotic tissue with overall sensitivity of 79%. SRS also helps in selection of patients who will be benefited from medical treatment with somatostatin analogues and to assess the therapeutic effects of somatostatin analogues in these patients.[39,40]
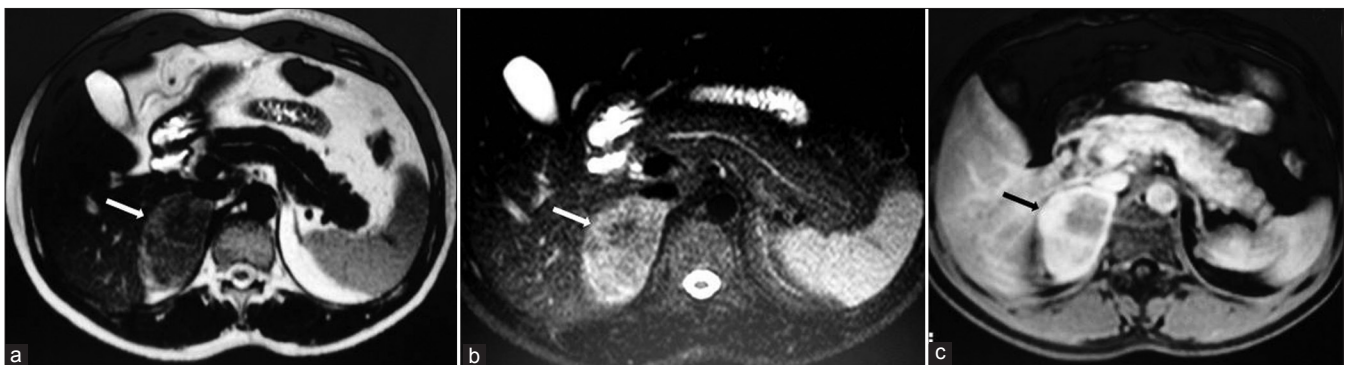

Figure 3: Pheochromocytoma. MRI abdomen in a 40-year-old male demonstrates a large right adrenal mass (arrow) appearing hypointense on axial T1-weighted image (a) and hyperintense on axial fat- suppressed T2-weighted image. (b) Postcontrast axial T1-weighted image (c) demonstrates marked but heterogeneous enhancement of the lesion. Clinically silent pheochromocytomas tend to be larger. The diagnosis of pheochromocytoma was confirmed on histopathological examination.

Anatomical and functional imaging in hyperthyroidism

Severe untreated hyperthyroidism (thyrotoxicosis) can be associated with elevated blood pressure; however, treatment of thyroid disorder usually lowers the blood pressure to normal. Most common forms of hyperthyroidism include diffuse toxic goiter (Graves' disease), toxic multinodular goiter (Plummer's disease), toxic adenoma, and subacute thyroiditis. CT and MRI are not routinely used to determine the cause of hyperthyroidism, although can be used selectively when sonography is inadequate or to detect the involvement of adjacent structures by the lesion.[41,42] Ultrasound is very sensitive, noninvasive imaging modality of choice for detecting thyroid lesions and distinguishing nodules from cysts. Combining high-resolution sonography with color Doppler and spectral analysis of the vasculature further improves the characterization of thyroid lesions [Figure 5].[43] In Graves' disease, the thyroid usually appears normal or moderately enlarged with hypoechoic or heterogeneous echotexture. Doppler study demonstrates diffuse parenchymal hypervascularity ("thyroid inferno") on color flow imaging and significantly high peak systolic velocities (PSV>70–100 cm/s) in inferior thyroid arteries

Figure 4: Pituitary macroadenoma. A 45-year-old female with features of acromegaly due to growth hormone producing pituitary macroadenoma. Postcontrast coronal (a) and sagittal (b) images of pituitary show a large moderately enhancing mass lesion in the sellar and suprasellar region

on spectral Doppler analysis. With toxic adenoma or multinodular goiter, sonogram demonstrates one or more thyroid nodules. In subacute thyroiditis, the gland is edematous and hypoechoic. On Doppler evaluation, hot nodules can also be differentiated from cold nodules with more prominent vascular patterns and significantly higher PSV values (>50–70 cm/s) in ipsilateral inferior thyroid artery.[44,45] Iodine-123 (^{123}I) and technetium-99m (^{99m}Tc) are used for thyroid scanning, which provide anatomic information on the type of lesion. A toxic multinodular goiter demonstrates an enlarged thyroid with multiple nodules and areas of increased and decreased uptake [Figure 6]. Graves' disease is associated with diffuse enlargement of both thyroid lobes, with an elevated uptake [Figure 7]. A toxic adenoma demonstrates a solitary hot nodule with suppression of function in the surrounding normal thyroid tissue. Subacute thyroiditis usually demonstrates very low ^{123}I isotope uptake.[46] A high correlation between radioisotope scan and color Doppler study has been established, which demonstrates that a scintigraphically hot nodule appears hypervascularized on color Doppler sonography with high PSV in ipsilateral inferior thyroid artery. Being an inexpensive, fast, and noninvasive imaging procedure as compared to radioisotope scan, the Doppler sonography is gaining importance over scintigraphy for the functional evaluation of thyroid disorders. Like ^{123}I isotope scan, Doppler sonography now also has a well-documented role in the management of patients with Graves' disease, as it helps in monitoring the patients with Graves' disease on anithyroid drug therapy. The important parameters evaluating the therapeutic efficacy in thyrotoxic patients are decrease in thyroid (Graves' disease) or nodular (toxic nodule) volume; decreased PSV in the inferior thyroid arteries and decreased radioiodine uptake (Graves' disease). Moreover, Doppler sonography is the investigation of choice in pregnancy and lactation where nuclear imaging is contraindicated.[44,45]
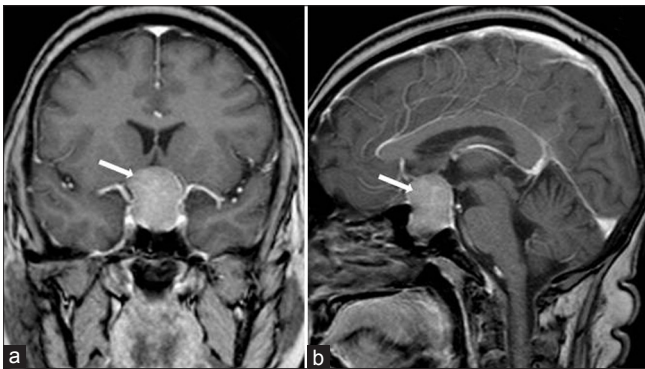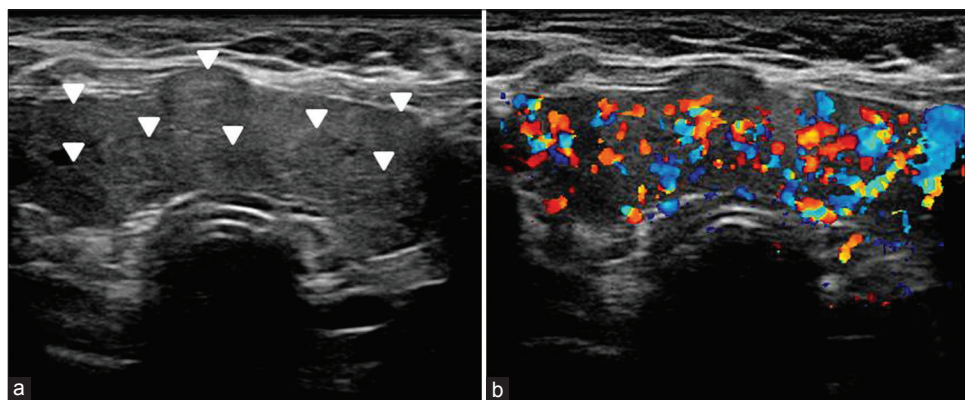

Figure 5: Multinodular goiter. Transverse gray-scale ultrasound (a) and color Doppler (b) neck, of a 50-year-old female patient, shows enlargement of both thyroid lobes and isthmus by multiple iso-hyperechoic solid nodules (arrowheads). Note, marked increase in vascularity within the gland. (Reproduced with permission from Indian Journal of Endocrinology and Metabolism)
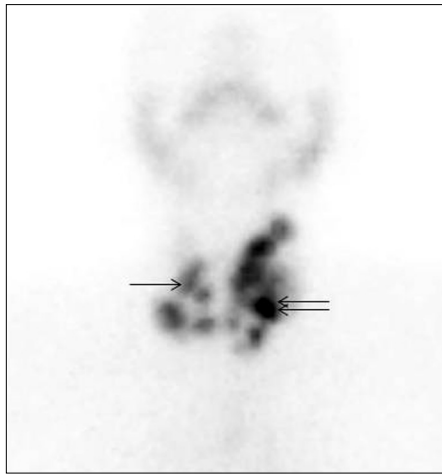
Figure 6: Multinodular goiter. ^{99m}Technetium pertechnetate (Tc-99m) scintigraphy of thyroid gland, of a 48-year-old female patient with multinodular goiter, shows multiple hot (double arrow) and cold nodules (single arrow) involving both lobes of the gland (left>right). (Reproduced with permission from Indian Journal of Endocrinology and Metabolism)
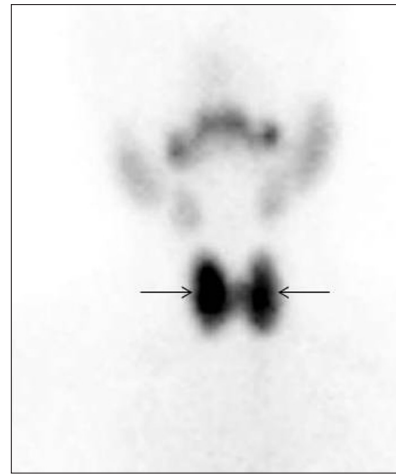

Figure 7: Grave's disease. Tc-99m scintigraphy image of thyroid gland, of a 37-year-old male patient who presented with neck mass and proptosis, demonstrates bilateral enlarged thyroid lobes with diffusely increased uptake of the tracer (arrow)

Anatomical and functional imaging in hyperparathyroidism

In patients with primary hyperparathyroidism, hypertension is observed in approximately 40% of cases and is related to hypercalcemia. In approximately 85% of cases, primary hyperparathyroidism is caused by a single adenoma. Multiple parathyroid gland disease (multiple adenomas and parathyroid hyperplasia) accounts for remaining 15% of cases and is associated with MEN type 1 and 2A.[47] Accurate preoperative localization of the hyperfunctioning parathyroid tissue is essential to aid successful surgical treatment. The imaging protocol usually consists of a combination of high-resolution ultrasound, radionuclide imaging, CT, and MRI. High-resolution ultrasound is the first line of investigation in evaluating neck in primary hyperparathyroidism in many institutions. The sensitivity of ultrasound in detecting parathyroid adenoma is 65–85%. Typical ultrasound feature of parathyroid adenoma varies from round or oval to elongated homogeneous hypoechoic nodule located close to thyroid gland or more inferiorly in para-tracheal and para-esophageal space. Large adenomas may show hemorrhage, cystic changes, and calcification. On color flow imaging, 90% parathyroid adenomas are hypervascular in nature.[48] Thin section, contrast-enhanced CT (CECT) is used for localization of parathyroid adenoma with sensitivity ranging from 46–87%. CECT demonstrates intensely enhancing nodule posterior to the thyroid gland.[49] MRI can be useful, particularly in cases of recurrent or persistent disease and in ectopic locations such as the mediastinum. On MRI, the hyperfunctioning parathyroid gland is iso-hypointense on T1-weighted image, hyperintense on T2-weighted image, and shows intense enhancement after administration of intravenous gadolinium. Intralesion hemorrhage may

produce hyperintense signal even on T1-weighted image.[50] Parathyroid scintigraphy is one of the most commonly employed imaging modalities for preoperative localization of hyperfunctioning parathyroid tissue. Its role has been well established in primary hyperparathyroidism (HPTH) but remains controversial in secondary HPTH (renal failure being the most common cause). The overall sensitivity of parathyroid scintigraphy in primary HPTH has been reported to be 88% for single adenomas, 30% for multiple adenomas, and 44% for multiple-gland hyperplasia. False positive scintigraphic finding, although uncommon, may be due to solid nodule in a solitary thyroid adenoma or a multinodular goiter. False negative rate, which is mainly attributed to small glandular size, is more among the patients with multiple parathyroid adenomas and multiple-gland hyperplasia than those with a single adenoma. The first radionuclide imaging technique widely used in the 1980s for localizing hyperfunctioning parathyroid tissue was the dual tracer substraction technique, which employed thallium-201(^{201}Tl-thallous chloride) that was taken up by both the thyroid and parathyroid, and technetium-99m (^{99m}Tc-sodium pertechnetate) that was taken up only by the thyroid tissue. In 1989, a new radionuclide, ^{99m}Tc sestamibi replaced ^{201}Tl because of superior image quality, favorable dosimetry and improved sensitivity. It was also observed that ^{99m}Tc sestamibi washes out more rapidly from the thyroid gland than from hyperfunctioning parathyroid tissue. Henceforth, preoperative technetium-99m (^{99m}Tc) sestamibi scintigraphy became a widely acceptable method to localize parathyroid adenomas. Scintigraphic protocols commonly used now days are single-phase dual-isotope subtraction imaging (technique includes subtraction of thyroid images obtained with iodine-123 (^{123}I) or ^{99m}Tc pertechnetate from those obtained with ^{99m}Tc sestamibi),

or dual-phase single-isotope imaging (the early-and delayed-phases show typically slower washout of ^{99m}Tc sestamibi from hyperfunctioning parathyroid glands as compared to the thyroid glands), or a combination of both to obtain a planar image. ^{99m}Tc sestamibi single photon emission computed tomography (SPECT) when combined with x-ray-based computed tomography (CT) provides three-dimensional functional information from SPECT and anatomic information from CT, and helps in preoperative detection and localization of the cause of primary hyperparathyroidism. Another myocardial perfusion agent, ^{99m}Tc tetrofosmin, also has been used for parathyroid scintigraphy, but with limited experiential data.[51,52] Role of PET scanning using ^{18}FDG or ^{11}C-methionine in detecting and localizing primary parathyroid adenoma has been established.[53] However, studies comparing these agents with ^{99m}Tc sestamibi are also needed. No studies to date have evaluated PET scanning in multiple parathyroid gland disease.

Conclusion

Modern imaging plays an important role in investigating endocrine hypertension. The use of an integrated functional and anatomical imaging approach to evaluate the pathologies causing endocrine hypertension has significant clinical relevance, particularly in the present era of minimally invasive surgery where accurate preoperative localization of the lesions is essential for safety and efficacy of surgery.

Acknowledgement

References

1. Kearney PM, Whelton M, Reynolds K, Muntner P, Whelton PK, He J. Global burden of hypertension: Analysis of worldwide data. Lancet 2005;365:217-23.
2. Stelios F, Agathocles T. Molecular genetic aspects and pathophysiology of endocrine hypertension. Hormones 2006;5:90-106.
3. Shilpan MP, Ravi KL, Tina IB, Tan LT, Beata B. Role of radiology in the management of primary aldosteronism. Radiographics 2007;27:1145-57.
4. Lockhart ME, Smith JK, Kenney PJ. Imaging of adrenal masses. Eur J Radiol 2002;41:95-112.
5. Blake MA, Kalra MK, Sweeney AT, Lucey BC, Maher MM, Sahani DV, et al. Distinguishing benign from malignant adrenal masses: Multi-detector row CT protocol with 10-min delay. Radiology 2006;238:578-85.
6. Peña CS, Boland GW, Hahn PF, Lee MJ, Mueller PR. Characterization of indeterminate (lipid-poor) adrenal masses: Use of washout characteristics at contrast-enhanced CT. Radiology 2000;217:798-802.
7. Young WF Jr. Clinical practice: The incidentally discovered adrenal mass. N Engl J Med 2007;356:601-10.
8. Alexandraki KI, Grossman AB. Adrenal incidentalomas: 'The rule of four'. Clin Med 2008;8:201-4.
9. Balkin PW, Hollifield JW, Winn SD, Shaff MI. Primary aldosteronism: Computerized tomography in pre-operative evaluation. S Med J 1985;159:1071-73.
10. Mayo-Smith WW, Boland GW, Noto RB, Lee MJ. State-of-the-art adrenal imaging. Radiographics 2001;21:995-1012.
11. Mayo-Smith WW, Lee MJ, McNicholas MM, Hahn PF, Boland GW, Saini S. Characterization of adrenal masses (< 5 cm) by use of chemical shift MR imaging: Observer performance versus quantitative measures. AJR Am J Roentgenol 1995;165:91-5.
12. Miller JC, Blake MA, Boland GW. Definitive characterisation of adrenal lesions. BMJ 2009;338:3092.
13. Science News. "Stealth Station" Imaging Tool Helps University Of Maryland Surgeons Treat Tumors Deep Within The Brain. ScienceDaily (Jan. 6, 2000).
14. Yoh T, Hosono M, Komeya Y, Im SW, Ashikaga R, Shimono T, et al. Quantitative evaluation of norcholesterol scintigraphy, CT attenuation value, and chemical-shift MR imaging for characterizing adrenal adenomas. Ann Nucl Med 2008;22:513-9.
15. Ilias I, Sahdev A, Reznek RH, Grossman AB, Pacak K, The optimal imaging of adrenal tumours: A comparison of different methods. Endocr Relat Cancer 2007;14:587-99.
16. Thompson GB, Young WF Jr. Adrenal incidentaloma. Curr Opin Oncol 2003;15:84-90.
17. Nieman L, Cutler GB Jr. Cushing's syndrome. In: DeGroot LJ, Besser M, Burger HG, et al, editors. Endocrinology, 3rd ed. Philadelphia, Pa: WB Saunders; 1995. p. 1741-69.
18. Sohaib SA, Hanson JA, Newell-Price JD, Trainer PJ, Monson JP, Grossman AB, et al. CT appearance of the adrenal glands in adrenocorticotrophic hormone-dependent Cushing's syndrome. AJR Am J Roentgenol 1999;172:997-1002.
19. Orth DN. Cushing's syndrome. N Engl J Med 1995;332:791-803.
20. Findling JW, Doppman JL. Biochemical and radiologic diagnosis of Cushing's syndrome. Endocrinol Metab Clin North Am 1994;23:511-37.
21. Kalgikar AM, Chandratreya SA, Goel A, Shrivastava M, Limaye US, Karvat A, et al. Inferior petrosal sinus sampling in the diagnostic evaluation of Cushing's syndrome: KEM experience. J Assoc Physicians India 2005;53:685-8.
22. Tabarin A, Valli N, Chanson P, Bachelot Y, Rohmer V, Bex-Bachellerie V, et al. Usefulness of somatostatin receptor scintigraphy in patients with occult ectopic adrenocorticotropin syndrome. J Clin Endocrinol Metab 1999;84:1193-202.
23. Allan CA, Kaltsas G, Perry L, Lowe DG, Reznek R, Carmichael D, et al. Concurrent secretion of aldosterone and cortisol from an adrenal adenoma - value of MRI in diagnosis. Clin Endocrinol (Oxf) 2000;53:749-53.
24. Soreide JA, Brabrand K, Thoresen SO. Adrenal cortical carcinoma in Norway, 1970-1984. World J Surg 1992;16:663-7.
25. Didolkar MS, Bescher RA, Elias EG, Moore RH. Natural history of adrenal cortical carcinoma: A clinicopathologic study of 42 patients. Cancer 1981;47:2153-61.
26. Arnaldi G, Angeli A, Atkinson AB, Bertagna X, Cavagnini F, Chrousos GP, et al. Diagnosis and complications of Cushing's syndrome: A consensus statement. J Clin Endocrinol Metab 2003;88:5593-602.
27. Peppercorn PD, Reznek RH. State-of-the-art CT and MRI of the adrenal gland. Eur Radiol 1997;7:822-36.
28. Lieberman SA, Eccleshall TR, Feldman D. ACTH-independent massive bilateral adrenal disease (AIMBAD): A subtype of Cushing's syndrome with major diagnostic and therapeutic implications. Eur J Endocrinol 1994;131:67-73.
29. Vezzosi D, Vignaux O, Dupin N, Bertherat J. Carney complex: Clinical

and genetic 2010 update. Ann Endocrinol (Paris) 2010;71:486-93.

30. Neumann HP, Bausch B, McWhinney SR, Bender BU, Gimm O, Franke G, et al. Germ-line mutations in nonsyndromic pheochromocytoma. N Engl J Med 2002;346:1459-66.

31. Maurea S, Cuocolo A, Reynolds JC, Tumeh SS, Begley MG, Linehan WM, et al. Iodine-131-metaiodobenzylguanidine scintigraphy in preoperative and postoperative evaluation of paragangliomas: Comparison with CT and MRI. J Nucl Med 1993; 34:173-9.

32. Furuta N, Kiyota H, Yoshigoe F, Hasegawa N, Ohishi Y. Diagnosis of pheochromocytoma using [^{123}I]-compared with [^{131}I]-metaiodobenzylguanidine scintigraphy. Int J Urol 1999;6:119-24.

33. Michael AB, Mannudeep KK, Michael MM, Dushyant VS, Ann TS, Peter RM, et al. Pheochromocytoma: An imaging chameleon. RadioGraphics 2004;24:S87-99.

34. Shulkin BL, Thompson NW, Shapiro B, Francis IR, Sisson JC. Pheochromocytomas: imaging with 2-[fluorine-18] fluoro-2-deoxy-D-glucose PET. Radiology 1999;212:35-41.

35. Hoegerle S, Nitzsche E, Altehoefer C, Ghanem N, Manz T, Brink I, et al. Pheochromocytomas: detection with ^{18}F DOPA whole-body PET-initial results. Radiology 2002;222:507-12.

36. Win Z, Rahman L, Murrell J, Todd J, Al-Nahhas A. The possible role of 68Ga-DOTATATE PET in malignant abdominal paraganglioma. Eur J Nucl Med Mol Imaging 2006;33:506.

37. Chaudhary V, Bano S. Imaging of the pituitary: Recent advances. Indian J Endocr Metab 2011;15:S216-23.

38. Nimsky C, Ganslandt O, von Keller B, Fahlbusch R. Intraoperative high-field MRI: Anatomical and functional imaging. Acta Neurochir Suppl 2006;98:87-95.

39. Ur E, Mather SJ, Bomanji J, Ellison D, Britton KE, Grossman AB, et al. Pituitary imaging using a labelled somatostatin analogue in acromegaly. Clin Endocrinol (Oxf) 1992;36:147-50.

40. Acosta-Gómez MJ, Muros MA, Llamas-Elvira JM, Ramírez A, Ortega S, Sabatel G, et al. The role of somatostatin receptor scintigraphy in patients with pituitary adenoma or post-surgical recurrent tumors. Br J Radiol 2005;78:110-5.

41. Miles J, Charles P, Riches P. A review of methods available for the identification of both organ- specific and non-organ-specific autoantibodies. Ann Clin Biochem 1998;35:19-47.

42. Loy M, Perra E, Melis A, Cianchetti ME, Piga M, Serra A, et al. Color-flow Doppler sonography in the differential diagnosis and management of amiodarone-induced thyrotoxicosis. Acta Radiol 2007;48:628-34.

43. Chaudhary V, Bano S. Imaging of the thyroid: Recent advances. Indian J Endocrinol Metab 2012;16:371-6.

44. Kumar KV, Vamsikrishna P, Verma A, Muthukrishnan J, Rayudu BR, Modi KD. Utility of color Doppler sonography in patients with Grave's disease. West Indian Med J 2009;58:566-70.

45. Summaria V, Salvatori M, Rufini V, Mirk P, Garganese MC, Romani M. Diagnostic imaging in throtoxicosis. Rays 1999;24:273-300.

46. Okosieme OE, Chan D, Price SA, Lazarus JH, Premawardhana LD. The utility of radioiodine uptake and thyroid scintigraphy in the diagnosis and management of hyperthyroidism. Clin Endocrinol (Oxf) 2010;72:122-7.

47. Fraker DL, Harsono H, Lewis R. Minimally invasive parathyroidectomy: Benefits and requirements of localization, diagnosis, and intraoperative PTH monitoring: Long-term results. World J Surg 2009;33:2256-65.

48. Gritzmann N, Koischwitz D, Rettenbacher T. Sonography of the thyroid and parathyroid glands. Radiol Clin North Am 2000;38:1131-45.

49. Tziakouri C, Eracleous E, Skannavis S, Pierides A, Symeonides P, Gourtsoyiannis N. Value of ultrasonography, CT and MR imaging in the diagnosis of primary hyperparathyroidism. Acta Radiol 1996;37:720-6.

50. Gotway MB, Higgins CB. MR imaging of the thyroid and parathyroid glands. Magn Reson Imaging Clin N Am 2000;8:163-82.

51. Tam HT, Wong YH, Cheung SK, Ngai WT, Choi PT. Parathyroid scintigraphy in patients with primary hyperparathyroidism: ^{99m}Tc sestamibi SPECT and SPECT/CT. J Hong Kong Col Radiol 2010;13:59-67.

52. Hedieh KE, Harvey AZ. Parathyroid scintigraphy in patients with primary hyperparathyroidism: ^{99m}Tc sestamibi SPECT and SPECT/CT. RadioGraphics 2008;28:1461-76.

53. Sundin A, Johansson C, Hellman P, Bergstrom M, Ahlstrom H, Jacobson GB, et al. PET and parathyroid L-[carbon-11] methionine accumulation in hyperparathyroidism. J Nucl Med 1996;37:1766-70.